



UNIVERSITY OF LEEDS

This is a repository copy of *Intracellularly degradable, self-assembled amphiphilic block copolycurcumin nanoparticles for efficient in vivo cancer chemotherapy*.

White Rose Research Online URL for this paper:
<http://eprints.whiterose.ac.uk/85193/>

Version: Accepted Version

Article:

Lv, L, Guo, Y, Shen, Y et al. (4 more authors) (2015) Intracellularly degradable, self-assembled amphiphilic block copolycurcumin nanoparticles for efficient in vivo cancer chemotherapy. *Advanced Healthcare Materials*, 4 (10). pp. 1496-1501. ISSN 2192-2640

<https://doi.org/10.1002/adhm.201500075>

Reuse

Unless indicated otherwise, fulltext items are protected by copyright with all rights reserved. The copyright exception in section 29 of the Copyright, Designs and Patents Act 1988 allows the making of a single copy solely for the purpose of non-commercial research or private study within the limits of fair dealing. The publisher or other rights-holder may allow further reproduction and re-use of this version - refer to the White Rose Research Online record for this item. Where records identify the publisher as the copyright holder, users can verify any specific terms of use on the publisher's website.

Takedown

If you consider content in White Rose Research Online to be in breach of UK law, please notify us by emailing eprints@whiterose.ac.uk including the URL of the record and the reason for the withdrawal request.



eprints@whiterose.ac.uk
<https://eprints.whiterose.ac.uk/>

DOI:

Article type: Communication

Intracellularly Degradable, Self-assembled Amphiphilic Block Copolycurcumin Nanoparticles for Efficient in vivo Cancer ChemotherapyLi Lv, Yuan Guo, Yuanyuan Shen, Jieying Liu, Wenjun Zhang,
Dejian Zhou* and Shengrong Guo*

Dr. L. Lv, Y. Shen, J. Liu, W. Zhang, Prof. Dr. S. Guo

School of Pharmacy

Shanghai Jiao Tong University

Shanghai, 200240, China

E-mail: serguo@sjtu.edu.cn or s.guo@leeds.ac.uk

Dr. Y. Guo, Dr. D. Zhou, Prof. S. Guo

School of Chemistry and Astbury Centre for Structural Molecular Biology

University of Leeds

Leeds, LS2 9JT, United Kingdom

E-mail: d.zhou@leeds.ac.uk

Chemotherapy is widely used in various cancer treatments. However, current cancer chemotherapy has a major limitation: lacking of specific targeting ability. As a result, it kills both cancerous and healthy cells, causing severe adverse side-effects and toxicity to patients which limits the dose regime and allows tumour to gain resistance. One approach to address this problem is the development of nanoscale drug delivery systems (NDDSs) which can exploit characteristic properties of tumour, such as the enhanced permeation and retention (EPR) effect,^[1] and over-expressed cell-surface receptors,^[2] to achieve targeted delivery.^[3] Despite significant research achievements, most of the current NDDSs, especially those in clinical trials or usage, e.g. drug encapsulated lipids vesicles or polymer micelles,^[4] polymer-drug conjugates, and albumin-based nanoparticles,^[5] mostly rely on passive targeting and generally lack the ability of active targeting. Moreover, drugs are mostly physically encapsulated or entrapped into the NDDSs, where drug release is mainly achieved via passive diffusion, making it difficult to achieve controlled release, a vital property for high therapeutic

efficacy. As a result, most of the drug payloads may have been released before reaching the target sites, leading to reduced therapeutic efficacy and causing adverse side-effects. Furthermore, most NDDSs also suffer from drawbacks such as low drug loading (e.g. antibody-drug conjugates) and/or burst release (e.g. micelles/liposomes). To date, none of the current NDDSs can satisfy all of the requirements of an “idea NDDS” outlined by Langer et al.^[3a]

To make best use of the advantages of current NDDSs (passive and active targeting delivery to tumour) and overcome their drawbacks (unnecessary and even harmful on-way drug release before entering tumour cells and/or only a small quantity of drugs together with the nano-carriers entering tumour cells) due to the physical incorporation or encapsulation of drugs in NDDSs, which often leads to uncontrolled drug release via diffusion, we take a new approach to prepare NDDSs which is based on so-called poly(active pharmaceutical ingredient) (PAPI) strategy where the APIs are incorporated into an intracellular cleavable polymer backbone (not physically incorporated in drug carriers) in combination with self-assembly characteristics of amphiphilic block copolymers. Here PAPI is defined as a polymer prepared by polycondensation of an API or its derivative having the same or similar bioactivity as a co- or sole- monomer. Considerable advantages here are that the physical-chemical properties of the PAPIs can be readily tailored by changing co-monomers or via chemical modifications. The PAPIs can be further made into various NDDSs where the API release can be controlled via stimuli triggered polymer degradation, overcoming the drawback of un-controlled, diffusion based drug release character commonly experienced in physically incorporated systems. In principle, any drug molecules/derivatives containing two or more functional groups (e.g. hydroxyl, amine or carboxylic acid) can be exploited to prepare PAPIs. Similarly, K. Uhrich reports on the chemical conjugation of antibiotics to polymers for localized and sustained drug release, achieved by forming covalent bonds between antibiotics and a pre-existing polymer or by developing novel antibiotic-containing polymers.^[6]

Curcumin (Cur) is extracted from turmeric as food additive or traditional medicine for centuries in China and India. It has been found that Cur has very low toxicity or even non-toxicity on healthy cells, but selective toxicity on many cancer cells. Cur can be used as chemo-preventive agent, chemo-/radio-sensitizer for tumour cells, as well as chemo-/radio-protector for healthy organs.^[7] However, Cur's clinical trials or in vivo applications are limited due to its poor water solubility, poor stability at physiological pH or under UV/Visible radiation. Many efforts have been made to overcome Cur's poor water solubility and instability, such as physical incorporation or encapsulation of Cur within a nanoparticle, conjugation with hydrophilic compounds and copolymerization with hydrophilic monomers.^[8-10] For example, the Shen's group has reported the first polycurcumins by condensation polymerization of curcumin with various hydrophilic PEGs. Such polycurcumin conjugates have the advantages of defined, high drug loading within the polymer backbones, leading to improved curcumin stability and tailored water-solubility.^[9] In this paper, Cur containing 2 hydroxyl groups each molecule is used as a model example to demonstrate our PAPI strategy. We envisaged that an amphiphilic biotin-PEG-b-poly(curcumin-dithiodipropionic acid) (Biotin-PEG-PCDA), consisting of a high molecular weight (MW) hydrophobic PCDA block and a long PEG block, would assemble into stable core-shell nanoparticles (NPs), resulting in greatly increased water-solubility and offering effective protection against recognition and uptake by the reticuloendothelial system, allowing for prolonged circulation and effective tumour targeted accumulation via the EPR effect. Moreover, the hydrophobic core made of PCDA should lead to high drug loading and providing effective protection for Cur against hydrolysis. The Biotin-PEG-PCDA NP should be stable during the blood transport but can readily release its API (Cur) once enters the target cancer cells/tissues triggered by the high intracellular glutathione (GSH, 1-10 mM v.s.~10 μ M in blood)^[11] and esterase^[12] contents. The over-expressed biotin receptors found on cancer cells can be exploited for effective, active cancer targeting.^[13] Importantly, the Biotin-PEG-PCDA NP can be loaded with a

second anticancer drug (e.g. doxorubicin, Dox) to exploit the synergy of combinational dual-drug therapy to further enhance in vivo anticancer efficacy.

The route to prepare the Biotin-PEG-PCDA NP is shown in **Figure 1** schematically. Cur was first copolymerized with dithiodi-propionic acid (DTDPA) to form a hydrophobic PCDA block, which was then coupled to a biotin-PEG to form the amphiphilic biotin-PEG-PCDA diblock copolymer. Details of the synthetic procedures and spectroscopic characterizations of the polymers were given in Supporting Information (SI, Figure S1 and S2, Table S1). The Biotin-PEG-PCDA and PEG-PCDA NPs were prepared by a simple O/W emulsion followed by solvent evaporation method without using emulsifiers or surfactants. For comparison, a poly(L-lactic acid anhydride ester)-b-PEG (Cur-PEG-PAE) NP loaded with Cur via physical encapsulation was also prepared.^[14] The biophysical parameters of the NPs were given in SI, Table S2.

The extremely low water-solubility of free Cur ($\sim 0.25 \mu\text{g/mL}$) has been a major limiting factor for its low bioavailability. As expected, the Biotin-PEG-PCDA and PEG-PCDA prepared here were found to have a much higher water-solubility, being 470 and 360 $\mu\text{g/ml}$ (corresponding to 127 and 84 $\mu\text{g/ml}$ equivalent of free Cur), respectively. This represents an enhanced solubility of > 500 fold (for Biotin-PEG-PCDA) over free Cur (SI, Table S1). Rapid degradation under physiological pH is another major factor limiting free Cur's bioavailability. This can be monitored by its characteristic absorption at ~ 420 nm in the UV-vis spectra. As shown in Figure S3 (SI), the UV-vis spectra of Biotin-PEG-PCDA in phosphate buffered saline (PBS, 10 mM phosphate, 150 mM NaCl, pH 7.4) over a course of 24 h were almost identical, with $< 5\%$ decrease of absorbance at 400 nm, indicating that the Biotin-PEG-PCDA was stable under such conditions. In contrast, a dramatic decrease ($> 50\%$) of absorbance at 420 nm was observed for free Cur in PBS over 30 min, illustrating a high instability. Therefore the formation of biotin-PEG-PCDA greatly improved the stability of Cur against

hydrolysis by > 500 fold under physiological conditions. The greatly increased solubility and stability of Cur afforded by the PAPI strategy should improve its bioavailability and hence in vivo anti-cancer efficacy.

As described above, GSH can be used as stimulus for triggered intracellular release. As shown in Figure S4 (SI), neither the DLS nor GPC profiles revealed any obviously changes when the Biotin-PEG-PCDA NPs were exposed to PBS without or with low GSH content (10 μ M), suggesting they were stable under such conditions over the investigated period (3 h), in agreement with the UV-vis data above. In contrast, significantly changes were observed in both the DLS and GPC profiles after exposure of the NPs to PBS containing 5 mM GSH (similar to the intracellular GSH level). The DLS profiles became wider with time, indicating the erosion and/or aggregation of the NPs, most likely due to the GSH triggered cleavage of the disulfide bonds in the Biotin-PEG-PCDA. The GPC curves further supported the degradation of the Biotin-PEG-PCDA over 3h. A LC-MS analysis of the Biotin-PEG-PCDA NP after treatment with PBS containing 5 mM GSH and esterase confirmed that the degraded specie is free Cur (MW 368.13). Together, these results revealed that the Biotin-PEG-PCDA NPs were stable under physiological conditions with low GSH content (e.g. 10 μ M, similar to that in blood transportation), but were readily cleaved to release the Cur based APIs once enter inside cancer cells, triggered by the high intracellular GSH and esterase contents.

The PCDA is fluorescent just like free Cur, so the cellular uptake of the Biotin-PEG-PCDA and PEG-PCDA NPs can be readily monitored by flow cytometry. Significant differences were observed for HeLa (human cervical cancer) cells after 24 h treatment with the two NPs: the PEG-PCDA NP treated cells displayed a much lower Cur fluorescence intensity, being only ~10% that of those treated with the Biotin-PEG-PCDA NP (Figure S6C, SI), suggesting that uptake of the Biotin-PEG-PCDA NP by HeLa cells was ~10 times as efficient as that of the PEG-PCDA NP. The result clearly validated biotin in active cancer

targeting, presumably via binding to cancer cell over-expressed biotin receptors for greatly enhanced uptake via receptor-binding mediated endocytosis. This cell uptake mechanism was further supported by the observation that HeLa cell uptake of the Biotin-PEG-PCDA NPs was significantly inhibited (by ~55%) by the presence of free biotin (2 mM), while uptake of the PEG-PCDA NP was effectively unaffected (SI, Figure S6D).

Human cervical (HeLa) and breast (EMT6) cancer cells were used to screen the cytotoxicities of the two NPs (Figure 2). Compared to the PEG-PCDA NP, the Biotin-PEG-PCDA NP exerted significantly higher cytotoxicities against both the HeLa and EMT6 cells. This result was consistent with a much higher cell uptake of the Biotin-PEG-PCDA NP observed in the flow cytometry measurement. It is worth noting that the PEG-PCDA NP was less cytotoxic than the Cur/PEG-PAE NP (or free Cur) despite both containing flexible and hydrophilic PEG chains which might hinder their cell uptake in a similar degree. However, the physically encapsulated Cur in the PEG-PAE NP could leak out of the carrier during the MTT assay, accounting for a relatively high cytotoxicity. This result implied that the PAPI based Biotin-PEG-PCDA NP should be less toxic towards healthy tissues as well as the blood than the physical encapsulated Cur/PEG-PAE NP, due to high stability under circulating conditions (no drug leak). Moreover, the low levels of biotin receptors in such cells should also minimize non-specific uptake. Another attractive feature of Cur-based chemotherapy is its selective cytotoxicity and low toxicity *in vivo*: Cur has been reported to have a much higher cytotoxicity against cancer cells over healthy cells,^[15a] and moreover, clinical trials have revealed Cur is safe to human even at a high dose of 8 g per day.^[7,15b]

The fluorescence of PCDA was not strong enough to monitor its *in vivo* biodistribution. We found however that doxorubicin (DOX), a fluorescent anticancer drug widely used in clinical treatment of various cancers, leukemia and Hodgkin's lymphoma could be readily loaded into the PEG-PCDA NP and used as fluorescence probe for its *in vivo* biodistribution.^[16] After intravenous injection in the EMT6 xenograft mouse model, free DOX was found to primarily

accumulate in liver, but rarely in the target tumour throughout the 24 h period (Figure 3A). In sharp contrast, significant amounts of the DOX/Biotin-PEG-PCDA NPs were accumulated in the target tumour, which were much higher than those found in other organs such as heart, spleen, lung or kidney. Moreover, the amount of the NPs accumulated in the tumour increased progressively over time, becoming even higher than that in liver after 24 h post injection, benefited from their abilities of both active (via cancer cell over-expressed biotin-receptors) and passive targeting (via prolonged circulation afforded by PEGylated NPs and hence efficient tumour targeted accumulation via the EPR effect). The tumour DOX concentration at 24 h post injection was 9 times higher than that of free DOX control, demonstrating a highly specific tumour targeting ability of the Biotin-PEG-PCDA NP. The PEG-PCDA NP also produced time dependent enrichment in the target tumour, presumably via the EPR effect mediated passive targeting, although the extent of the NP accumulation was not as high as that for the Biotin-PEG-PCDA NP (Figure 3B and 3C). A significant 2.4 fold higher tumour accumulation for the biotinylated over the non-biotinylated NP clearly confirmed that biotin was a highly effective in vivo tumour targeting ligand.

The in vivo anti-cancer efficacy of the Biotin-PEG-PCDA NP was evaluated on EMT6 xenografted mouse model via intravenous injection (**Figure 4**). The body weights of all groups increased gradually throughout the course of treatment, showing no significant differences among different groups, suggesting no significant toxicity. It was exciting that treatments with the Biotin-PEG-PCDA NPs yielded the highest the inhibition rate of tumour growth (IRT, 79%), higher than those of the PEG-PCDA and Cur/PEG-PAE NPs and also free Cur (with IRTs of 69%, 60% and 32% respectively), demonstrating a high tumour growth inhibition by the Biotin-PEG-PCDA NP treatment. In fact, the tumour size effectively showed no growth once being treated with the Biotin-PEG-PCDA NP, while all other groups showed considerable tumour size growth. Interestingly, despite displaying a lower in vitro cytotoxicity against the EMT6 cells than the Cur/PEG-PAE NP, the PEG-PCDA NP actually produced a

higher tumour growth inhibition efficacy *in vivo*. This result highlighted the advantage of PAPI strategy over physical encapsulation: the Cur payloads in the later could leak out of the NP carrier before reaching the tumour target, leading to side-effect and reduced therapeutic efficacy *in vivo*. In contrast, the PAPI based PEG-PCDA NP could overcome such uncontrolled, diffusion based drug release drawback and only released its drug payloads after entering into target cancer cells, leading to high *in vivo* therapeutic efficacy.

The *in vivo* effects of the Biotin-PEG-PCDA NP on apoptosis, proliferation, and angiogenesis properties were further investigated by histological and immunohistochemical analyses. Our results revealed that the Biotin-PEG-PCDA NP were highly effective in inducing tumour cell apoptosis and inhibiting cell proliferation by providing effective anti-angiogenesis properties (see SI, Figure S7).

The facts that the DOX loaded Biotin-PEG-PCDA NP displayed highly specific tumour targeted accumulation (Figure 3) and released its drug payloads after entering into cancer cells make it ideal to exploit the synergy of combinational dual-drug chemotherapy to maximize treatment efficacy. Indeed, the DOX loaded Biotin-PEG-PCDA NP displayed a remarkably high *in vivo* anticancer efficacy on ETM6 tumour in mice, which was better than that of the Biotin-PEG-PCDA NP alone (Figure 5). After 6 days of treatment, the tumour size of the dual-drug treated group shrank by ~30% from the starting point of treatment. In contrast, all control groups yielded significant tumour size growths of ~700, ~240 and ~160% after treatment with saline, free DOX and DOX + biotin-PEG-PCDA polymer physical mixture, respectively. This confirmed that the DOX loaded biotin-PEG-PCDA NP was far more effective than the simple physical mixture of the drugs (Figure 5B), highlighting the value of our PAPI based nanomedicine in improving therapeutic efficacy *in vivo*. **The significantly improved *in vivo* anticancer efficacy obtained for the DOX loaded biotin-PEG-PCDA NP may be originated from the synergy of the combined DOX-Cur dual-drug therapy similar to that reported by the Shen group^[10a] as well as by us.^[10b]** It should be noted that despite

numerous studies, most cancer chemotherapy nanomedicines have only managed to inhibit,^[17] but not reverse the tumour growth unless being combined with other treatment modalities.^[18]

The fact that the DOX-loaded biotin-PEG-PCDA NP has successfully reduced the tumour size by 30% after 6 days of treatment demonstrated a real promise of curing cancer by chemotherapy in vivo. In particular, it can be further loaded with other anticancer drugs to exploit the synergy of combinational dual-/multi- drug therapy to maximize the efficacy. Importantly, all mice groups showed similar levels of continuing body weight gains throughout the course of treatment, implying no significant toxicity effect of the PAPI NPs (SI, Figure S8).

In summary, we have developed a new strategy for effective, targeted in vivo cancer chemotherapy by combining the PAPI and NDDS strategies using Cur as a model example. We have overcome the poor solubility and low stability of free Cur in physiological buffers, a key barrier limiting its in vivo efficacy, by coupling Cur into a disulfide-linked, hydrophobic polymer backbone appended with a terminal PEG-biotin. As a result, the drug's own hydrophobicity has been successfully exploited to initiate stable NP assembly, leading to greatly improved solubility and stability. The resulting PAPI NP offered high drug loading (~27% weight), good stability in physiological buffer, Biotin-mediated high cell uptake and intra-cellular high GSH-/esterase triggered release, overcoming the drawbacks of low drug loading, uncontrolled drug release or leakage during transport often experienced by physical encapsulation based nanomedicines. In particular, the biotinylated PAPI NP displayed a greatly increased, specific, tumour-targeted accumulation, leading to impressive in vivo antitumour efficacy benefited from both the active and passive targeting abilities. The high in vivo anticancer efficacy was found to originate from high degrees of induced apoptosis, anti-angiogenic activity and inhibition of cell proliferation. More importantly, the Biotin-PEG-PCDA NP can be loaded with DOX to exploit the synergy of combinational dual chemotherapy, leading to even higher in vivo anticancer efficacy without obvious toxicity.

Supporting Information

Supporting Information is available from the Wiley Online Library.

Acknowledgements

This work was supported by National Natural Science Foundation of China (NSFC, Grant No.81171439), National Basic Research Program of China (973 Program, Grant 2010CB529902), the National Key Technology R & D Program of the Ministry of Science and Technology (2012BAI18B01) and the European Union FP7 via a Marie Curie International Incoming Fellowship to S.G. (Grant No: PIIF-GA-2012-331281). We also thank the Instrumental Analysis Center of Shanghai Jiao Tong University for technical support in TEM and LC-HRMS analysis.

Received: ((will be filled in by the editorial staff))

Revised: ((will be filled in by the editorial staff))

Published online: ((will be filled in by the editorial staff))

-
- [1] a) Y. Matsumura, H. A. Maeda, *Cancer Res.* **1986**, 46, 6387-6392. b) S. Yu, Y. Zhang, X. Wang, X. Zhen, Z. Zhang, W. Wu, X. Jiang. *Angew. Chem. Int. Ed.* **2013**, 52, 7272-7277.
- [2] C. E. Ashley, E. C. Carnes, G. K. Phillips, D. Padilla, P. N. Durfee, P. A. Brown, T. N. Hanna, J. Liu, B. Phillips, M. B. Carter, N. J. Carroll, X. Jiang, D. R. Dunphy, C. L. Willman, D. N. Petsev, D. G. Evans, A. N. Parikh, B. Chackerian, W. Wharton, D. S. Peabody, C. J. Brinker, *Nat. Mater.* **2011**, 10, 389-397.
- [3] a) D. Peer, J. M. Karp, S. Hong, O. C. Farokhzad, R. Margalit, R. Langer, *Nat. Nanotech.* **2007**, 2, 751-760. b) Y. Namiki, T. Fuchigami, N. Tada, R. Kawamura, S. Matsunuma, Y. Kitamoto, M. Nakagawa, *Acc. Chem. Res.* **2011**, 44, 1080-1093. c) J. You, P. Guo, D. Auguste, *Angew. Chem. Int. Ed.* **2013**, 52, 4141-4146.

- [4] T. Y. Kim, D. W. Kim, J. Y. Chung, S. G. Shin, S. C. Kim, D. S. Heo, N. K. Kim, Y. J. Bang, *Clin. Cancer Res.* **2004**, 10, 3708-3716.
- [5] A. O. Elzoghby, W. M. Samy, N. A. Elgindy, *J. Control. Release* **2012**, 157, 168-182.
- [6] N. D. Stebbins, M. A. Ouimet, K. E. Uhrich, *Adv. Drug Deli. Rev.* **2014**, 78, 77-87
- [7] J. Liu, S. Chen, L. Lv, L. Song, S. Guo, S. Huang, *Cur. Pharm. Design.* **2013**, 19, 1974-1994
- [8] A. Safavy, K. P. Raisch, S. Mantena, L. L. Sanford, S. W. Sham, N. R. Krishna, J. A. Bonner, *J. Med. Chem.* 2007, 50, 6284-6288
- [9] H. Tang, C. J. Murphy, B. Zhang, Y. Shen, E. A. Van Kirk, W. J. Murdoch, M. Radosz, *Biomaterials* **2010**, 31, 7139-7149
- [10] a) H. Tang, C. J. Murphy, B. Zhang, Y. Shen, M. Sui, E. A. Van Kirk, X. Feng, W. J. Murdoch, *Nanomedicine*, 2010, 5, 855-65. b) W. Tian, J. Liu, Y. Guo, Y. Shen, D. Zhou, S. Guo, *J. Mater. Chem. B.* **2015**, 3, 1204-1207.
- [11] R. Cheng, F. Feng, F. Meng, C. Deng, J. Feijen, Z. Zhong, *J. Control. Release* **2011**, 152, 2-12.
- [12] C. Huggins, S. H. Moulton, *J. Exp. Med.* **1948**, 88, 169-179.
- [13] a) G. Russell-Jones, K. McTavish, J. McEwan, J. Rice, D. Nowotnik, *J. Inorg. Biochem.* **2004**, 98, 1625-1633. b) L. Cao, G. Hettiarachchi, V. Briken, L. Isaacs, *Angew. Chem. Int. Ed.* **2013**, 52, 12033-12037.
- [14] a) L. Lv, Y. Shen, M. Li, X. Xu, M. Li, S. Guo, S. Huang, *J. Biomed. Nanotech.* **2014**, 10, 324-335. b) L. Lv, Y. Shen, J. Liu, F. Wang, M. Li, A. Guo, Y. Wang, D. Zhou, S. Guo, *J. Biomed. Nanotech.* **2014**, 10, 179-193.
- [15] a) R. Chang, L. Sun, T. J. Webster, *Int. J. Nanomedicine*, **2014**, 9, 461-465. b) A. L. Cheng, C. H. Hsu, J. K. Lin, M. M. Hsu, Y. F. Ho, T. S. Shen, J. Y. Ko, J. T. Lin, B. R. Lin, W. Ming-Shiang, H. S. Yu, S. H. Jee, G. S. Chen, T. M. Chen, C. A. Chen, M. K.

- Lai, Y. S. Pu, M. H. Pan, Y. J. Wang, C. C. Tsai, C. Y. Hsieh, *Anticancer Res.* **2001**, 24, 2895-2900.
- [16] a) V. Bagalkot, O. C. Farokhzad, R. Langer, S. Jon, *Angew. Chem. Int. Ed.* **2006**, 45, 8149-8152. b) L. Song, V. H.B. Ho, C. Chen, Z. Yang, D. Liu, R. Chen, D. Zhou, *Adv. Healthcare Mater.* **2013**, 2, 275-280.
- [17] a) Q. Sun, X. Sun, X. Ma, Z. Zhou, E. Jin, B. Zhang, Y. Shen, E. A. Van Kirk, W. J. Murdoch, J. R. Lott, T. P. Lodge, M. Radosz, Y. Zhao, *Adv. Mater.* **2014**, 26, 7615–7621. b) Y. Tian, X. Jiang, X. Chen, Z. Shao, W. Yang, *Adv. Mater.* **2014**, 26, 7393–7398. c) Y. Chen, Q. Meng, M. Wu, S. Wang, P. Xu, H. Chen, Y. Li, L. Zhang, L. Wang, J. Shi, *J. Am. Chem. Soc.* **2014**, 136, 16326–16334.
- [18] J.-H. Lee, K.-J. Chen, S.-H. Noh, M. A. Garcia, H. Wang, W.-Y. Lin, H. Jeong, B. J. Kong, D. B. Stout, J. Cheon, H.-R. Tseng, *Angew. Chem. Int. Ed.* **2013**, 52, 4384-4388.

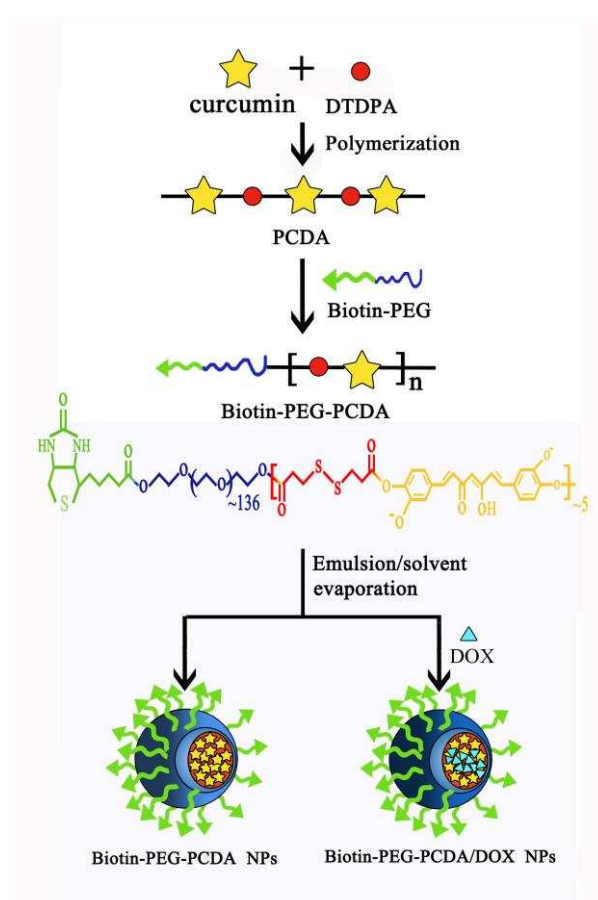


Figure 1. Schematic route towards the preparation of Biotin-PEG-PCDA and Dox loaded Biotin-PEG-PCDA NPs. DTAPA: dithiodipropionic acid; PCDA: poly(curcumindithio dipropionic acid).

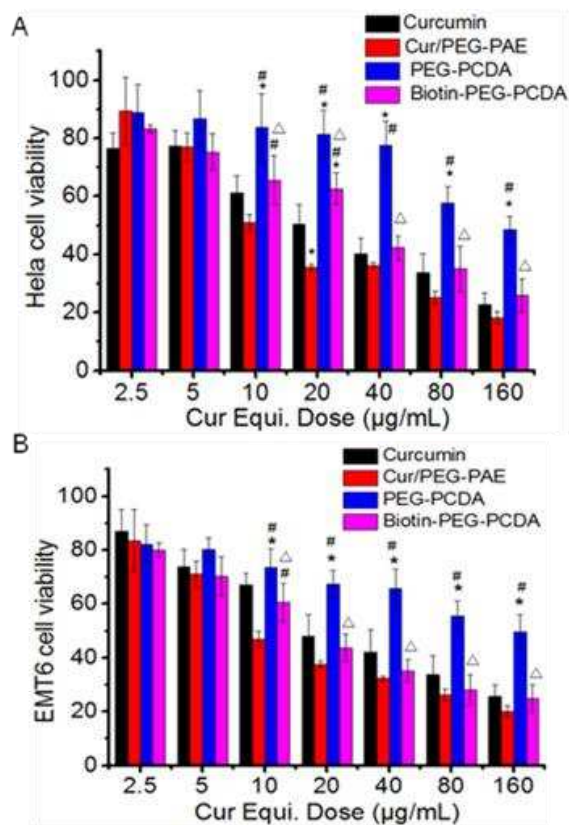


Figure 2. Cell viabilities of HeLa (A) and EMT6 cells (B) after treatment with the Biotin-PEG-PCDA, PEG-PCDA and Cur/PEG-PAE NPs and free Cur for 72 h. Data are given in mean \pm SD (n=10). *: significant difference compared to free Cur ($p < 0.05$); #: significant difference compared to the Cur/PEG-PAE NP ($p < 0.05$), Δ : significant difference compared to the PEG-PCDA NP ($p < 0.05$).

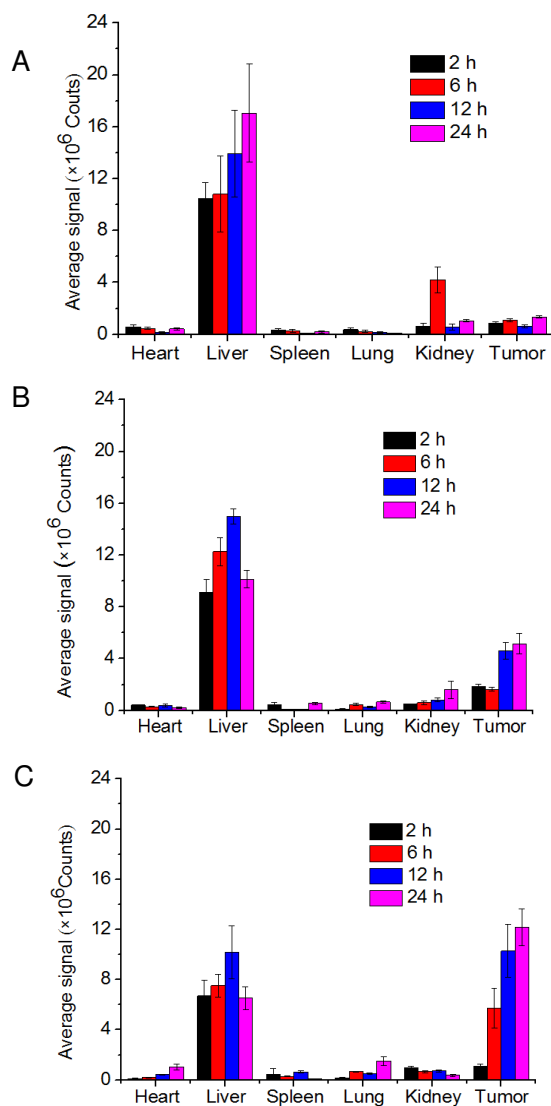


Figure 3. Bio-distribution of DOX (expressed as the average signal) in major organs (heart, liver, spleen, lung and kidney) and tumour tissue of EMT6 tumour bearing Kunming mice after 2, 6, 12 or 24 h intravenous injection of, (A) Free DOX·HCl; (B) DOX-loaded PEG-PCDA NP; and (C) DOX-loaded Biotin-PEG-PCDA NP.

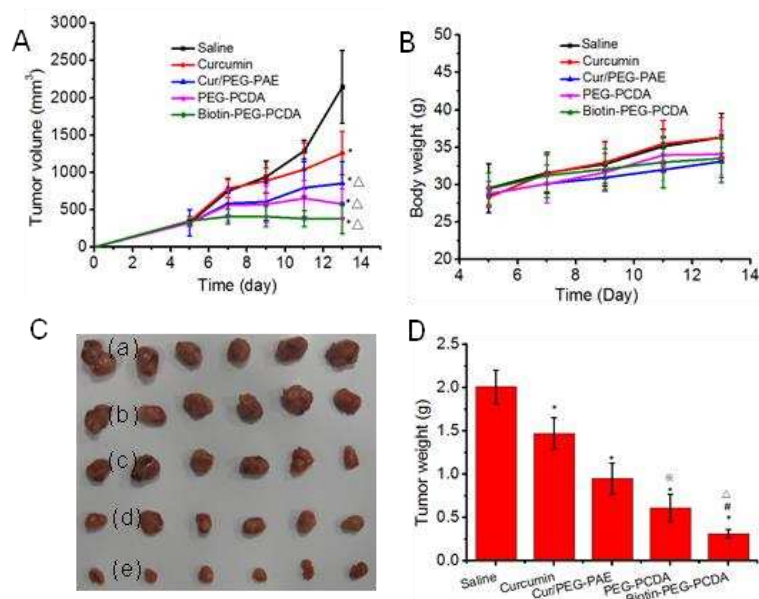


Figure 4. In vivo antitumour activity of the Biotin-PEG-PCDA NP on EMT6 carcinoma xenografted mice model (Cur or equivalent dose: 10 mg/kg). (A) The tumour volume growth curves, *: $p < 0.01$ compared to negative control; Δ : $p < 0.01$, compared to free Cur; (B) Mice body weight growth curves; (C) Photographs of EMT6 tumours in Kunming mice after treatment with saline (a), free Cur (b), Cur/PEG-PAE NP (c), PEG-PCDA NP (d) or Biotin-PEG-PCDA NP (e); (D) Weights of the EMT6 tumours in Kunming mice after 9 day treatment (significant difference, *: $p < 0.01$ compared to saline group; #: $p < 0.01$ compared to Cur/PEG-PAE group; \times : $p < 0.05$ compared to Cur/PEG-PAE; Δ : $p < 0.05$, compared to PEG-PCDA group).

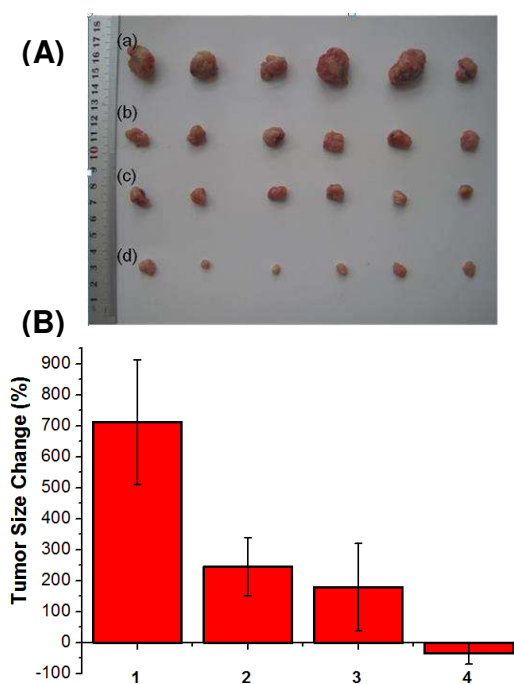


Figure 5. In vivo antitumour activity of the DOX loaded Biotin-PEG-PCDA NP on EMT6 xenografted mice model. (A) Photos of the EMT6 tumours in Kunming mice after treatment with saline (a), free DOX (b), DOX + Biotin-PEG-PCDA polymer (c) and DOX loaded Biotin-PEG-PCDA NP (d). The dosage of DOX was 2 mg/kg and the dosage of Biotin-PEG-PCDA was 14.7 mg/kg (equivalent of 4 mg/kg of Cur). (B) Comparison of the tumour size changes after 6 day treatment: (1) saline; (2) free DOX, (3) DOX + Biotin-PEG-PCDA polymer, and (4) DOX loaded Biotin-PEG-PCDA NP. Error bars represent the standard deviation (n = 6).

The table of contents

Intracellularly degradable, self-assembled amphiphilic Biotin-PEG-PCDA nanoparticles that display excellent *in vivo* anticancer efficacy benefitted from their high tumor accumulation and stimuli-triggered intracellular drug release are developed. They can be loaded with other anticancer drugs (e.g. doxorubicin) to exploit the synergy of combinational dual-drug therapy to further enhance *in vivo* anticancer efficacy.

Keyword

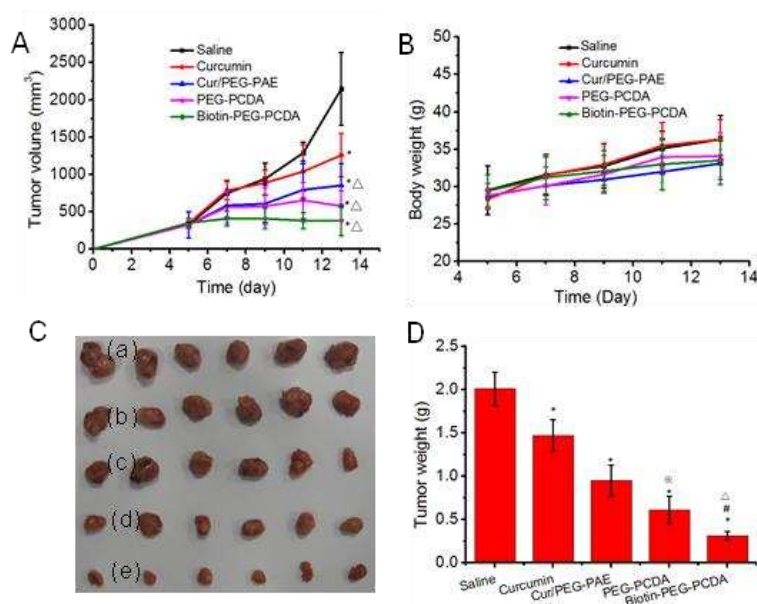
nanomedicine, self-assembly, drug delivery, cancer therapy, curcumin, polycurcumin

Li Lv, Yuan Guo, Yuanyuan Shen, Jieying Liu, Wenjun Zhang, Dejian Zhou* and Shengrong Guo*

Title:

Intracellularly Degradable, Self-assembled Amphiphilic Block Copolycurcumin Nanoparticles for Efficient *in vivo* Cancer Chemotherapy

ToC figure



Supporting Information

Intracellularly Degradable, Self-assembled Amphiphilic Block Copolycurcumin Nanoparticles for Efficient *in vivo* Cancer Chemotherapy

Li Lv, Yuan Guo, Yuanyuan Shen, Jieying Liu, Wenjun Zhang,
Dejian Zhou* and Shengrong Guo*

Part1: Experimental Section

1.1 Materials. 3, 3'-dithiodipropionic acid (DTDPA), N, N'-dicyclohexylcarbodiimide (DCC), 4-dimethylaminopyridine (DMAP), glutathione (GSH), methoxyl poly (ethylene glycol) (mPEG, Mw = 5000), poly (ethylene glycol) (PEG, Mw = 6000) and biotin were obtained from Aladdin chemistry Co., Ltd. (Shanghai, China). Cur and Doxorubicin hydrochloride were purchased from Alfa-Aesar. Dulbecco's modified eagle's medium (DMEM) was purchased from Invitrogen Corporation (Grand Island, USA). Penicillin-streptomycin, fetal bovine serum (FBS), 0.25% (w/v) trypsin, 0.03% (w/v) EDTA solution, phosphate buffer solution (PBS), 3-(4,5-dimethylthiazol-2-yl)-2,5-diphenyl-tetrazolium bromide (MTT) and dimethyl sulfoxide (DMSO) were purchased from Solarbio science & technology (Beijing, China). Propidium iodide (PI) was purchased from Solarbio science technology & (Beijing, China). RNase A was purchased from Beyotime (Suzhou, China).

1.2 Polymer Synthesis

1.2.1 Synthesis of PCDA. Cur (1.000 g), DTDPA (0.571 g), DCC (1.150 g) and DMAP (0.100 g) were dissolved in 40 mL anhydrous dichloromethane. The resulting solution was stirred at room temperature for 24 h. After removal of the formed dicyclohexyl urea (DCU) by filtration, the obtained filtrate was added into an excess of anhydrous ether (1000 mL) to produce a precipitate. The precipitate was further treated by multiple precipitations from dichloromethane with anhydrous ether, and finally dried under vacuum to yield a deep yellow solid product (PCDA, 0.95g, yield ~60%).

1.2.2 Synthesis of PEG-PCDA. PCDA (0.90 g), mPEG (1.125 g), DCC (46 mg) and DMAP (2.74 mg) were dissolved in 40 mL anhydrous dichloromethane. This solution was stirred at room temperature for 24 h. After filtration to remove the formed DCU, the filtrate

was added into an excess of anhydrous ether to produce a precipitate. The precipitate was dissolved in water and dialyzed against deionized water for 24 h with a dialysis membrane (MW cut-off of 6000 Da). The product (PEG-PCDA) was obtained by lyophilization and kept under dry conditions (1.76g, yield ~87%).

1.2.3 Synthesis of Biotin-PEG-PCDA. Biotin (0.066 g), PEG6000 (1.350 g), DCC (0.111g), DMAP (9.9 mg) were dissolved in 40 mL anhydrous dichloromethane. This solution was stirred at room temperature for 24 h. After filtration to remove the formed DCU, the filtrate was added into an excess of anhydrous ether to produce a precipitate. The precipitate was further treated by multiple precipitations from dichloromethane with anhydrous ether and dried under vacuum to yield the Biotin-PEG as a white solid (1.27 g, yield~90%).

PCDA (0.90 g), Biotin-PEG (0.337 g), DCC (22 mg) and DMAP (2 mg) were dissolved in 40 mL anhydrous dichloromethane. The resulting solution was stirred at room temperature for 24 h. After filtration to remove DCU, the filtrate was added into an excess of anhydrous ether to produce a precipitate. The precipitate was dissolved in water and dialyzed against deionized water for 24 h with a dialysis membrane (MW cut-off of 6000 Da). The Biotin-PEG-PCDA was obtained as a dry powder after lyophilization (1.03g, yield~83%).

1.3 NMR and GPC measurements. $^1\text{H-NMR}$ spectra were measured on a Varian-Mercury Plus (400 MHz) spectrometer with CDCl_3 as solvent. The chemical shifts were calibrated using tetramethylsilane as an internal standard. GPC measurements were performed at 40 °C on a Waters HPLC system equipped with a model 1525 binary HPLC pump, a model 2414 refractive index detector and a series of Styragel[®] columns (HR₃ and HR₄). Tetrahydrofuran was used as an eluent at a flow rate of 1.0 mL/min and the MWs were calibrated with polystyrene standard.

1.4 Solubility and stability tests. Solubility of free Cur or the PCDA based polymers was determined by adding an excess of Cur or polymers into distilled water. The mixture was vortexed for 10 min to reach solubility equilibrium and centrifuged at 10000 rpm for 5 min. The supernatant was separated and diluted with DMSO for UV measurement at 400 nm (for polymers) or 420 nm (for Cur) on a HITACHI U-2910 spectrophotometer. Free Cur or polymer DMSO solutions were used to generate a standard curve. Stability of Cur or polymers in aqueous media at physiological pH of 7.4 was studied by monitoring the UV-visible absorption spectra of Cur or polymers in aqueous media.

1.5 Preparation of PEG-PCDA and Biotin-PEG-PCDA NPs. 50 mg of the PEG-PCDA or Biotin-PEG-PCDA was dissolved in 4 mL dichloromethane (DCM). Afterwards, 6 mL of deionized water was slowly added into the DCM solution and then sonicated at 200 w for 2 min to form an O/W emulsion, the power was pulsed for 5s every 30 s to minimize temperature increases. The O/W emulsion was further diluted with 30 mL of deionized water and then magnetically stirred for 20 min at room temperature. After which the DCM was evaporated by rotary evaporation at 30 °C. The PEG-PCDA or Biotin-PEG-PCDA NPs aqueous solution was obtained after centrifugation at 4000 rpm for 20 min to remove any aggregated particles.

1.6 TEM imaging The morphology of PEG-PCDA or Biotin-PEG-PCDA NPs was observed by transmission electron microscopy (TEM, JEM-2010/INCA OXFORD). A drop of diluted solution of PEG-PCDA or Biotin-PEG-PCDA NPs was placed on a copper grid, stained with 2% phosphotungstic acids and dried before measurement.

1.7 Sizes and zeta potential measurements. The particle size and size distribution of PEG-PCDA or Biotin-PEG-PCDA NPs were determined by dynamic light scattering (DLS) using a Malvern Instrument Zeta size Nano-S at a detection angle of 173°. All measurements were repeated three times at room temperature. The zeta potential was measured by the light scattering method using a BC Haven instruments corporation 90 plus particle size analyzer.

1.8 Curcumin content measurement. Cur loading content was investigated as previously described,³¹ the Cur loading content in PEG-PCDA or Biotin-PEG-PCDA NPs was calculated from the ¹H-NMR spectra using the following equation:

$$\text{Cur Loading (\%)} = \frac{\text{amount of curcumin incorporated into polymer}}{\text{weight of the polymer}} \times 100\%$$

1.9 GSH triggered Degradation test. The degradation test of Biotin-PEG-PCDA was carried out in phosphate buffered solution (PBS, pH 7.4), PBS with 10 μM GSH, and PBS with 5 mM GSH, respectively. 10 mg of Biotin-PEG-PCDA was dissolved in 10 mL of solution and stirred at 37 °C. At certain time intervals, aliquots of the solution were withdrawn for DLS measurement and then lyophilized. The lyophilized product was dissolved in THF for GPC measurement.

1.10 LC-HRMS Analysis of the Biotin-PEG-PCDA NP degradation

Freeze-dried Biotin-PEG-PCDA NP powder (~10 mg) was dissolved in PBS with 5 mM GSH and 100 U esterase. The obtained clear solution was then incubated at 37 °C on a shaker for 24 h. After that, the solution was freeze-dried and the resulting dry powder was directly dissolved in chromatographic grade acetonitrile and centrifuged at 13,000 rpm for 30 mins. The clear supernatant on the top was then analysed by LC-HRMS using the conditions below.

LC-HRMS was performed on a Waters ACQUITY UPLC system equipped with a binary solvent delivery manager and a sample manager, coupled with a Waters Micromass Q-TOF Premier Mass Spectrometer equipped with an electrospray interface (Waters Corporation, Milford, MA) at the Instrumental Analysis Center of Shanghai Jiao Tong University under the following conditions:

Column: Acquity BEH C18 column (100 mm × 2.1 mm, Waters, Milford, USA). Solvent: the column was maintained at 45 °C and eluted with gradient solvent **A:B** mixture from 95:5 to 0:100 at a flow rate of 0.40 mL/min, where **A** is aqueous formic acid (0.1% formic acid) and **B** is acetonitrile with 0.1% (v/v) formic acid. UV detection wavelength: 225 nm; Injection Volume: 3.00 µL; Column temperature: 45.0 °C.

Polarity: positive (+): Capillary voltage: 3.0 kV; Sampling cone: 35 V; Collision energy: 4 eV; Source temperature: 100 °C, Desolvation temperature: 300 °C; Desolvation gas: 500 l/hr, Scan range: m/z 50~1000, Scan time: 0.3 s, Inter-scan time: 0.02 s.

Polarity: negative (-): Capillary voltage: 2.6, Sampling cone: 55 V, Collision energy: 4 eV, Source temperature: 100 °C, Desolvation temperature: 300 °C, Desolvation gas: 500 l/hr, Scan range: m/z 50~1000, Scan time: 0.3 s, Inter-scan time: 0.02 s.

1.11 Cellular uptake. HeLa cells were seeded at a density of 1.5×10^5 cells/mL (2 mL DMEM/well) in 6-well plates and allowed to adhere to the plates for 24 h. After removal of DMEM (with 1% penicillin-streptomycin and 10% FBS), 2 mL of the fresh DMEM with 25 µg/mL (equivalent Cur) of the PEG-PCDA or Biotin-PEG-PCDA NPs was added into each well. At the designated time points (after incubation for 0.5, 2, 4, and 24 h), the cells were washed three times with ice-cold PBS, collected by centrifugation and resuspended in 0.5 mL PBS. The amount of uptake of NPs was measured on a flow cytometer (BD LSRFortessa, Becton Dickinson) using a 405 nm argon laser for excitation and a 515-545 nm emission band-pass filter to detect the fluorescence of Cur. To investigate if free biotin could hinder the biotin receptor mediated endocytosis, HeLa cells were pre-incubated with 2 mM free biotin for 0.5 h before the cells were exposed to the PEG-PCDA or Biotin-PEG-PCDA NPs.

1.12 MTT assay. The in vitro cytotoxicity assays were performed following our earlier procedures.^[2] Briefly, HeLa or EMT6 cells in their logarithmic growth regime were seeded and incubated in 96-well plates at a density of 5000 cells/well in 200 μ L DMEM for 24 h, then, the culture medium in each well was carefully replaced by 200 μ L of fresh DMEM containing various concentrations of the NPs or free Cur ranged from 2.5 to 160 μ g/mL. After 72 h incubation, followed by removal of the media, each well was added with 180 μ L fresh DMEM and 20 μ L of PBS containing 5 mg/mL MTT. The media were discarded after 4 h incubation, and 200 μ L of DMSO was added into each well to dissolve the formed formazan crystals. The absorbance at 570 nm was recorded on an ELISA plate reader (Varioskan Flash). Cell viability of untreated cells (incubated with DMEM) is defined as 100%. Each experiment was done with ten parallel samples. Cells incubated in DMEM containing 0.1% DMSO, 3, 3'-dithiodipropionic acid, PEG, biotin, or PAE-b-PEG, were also as controls.

In the following animal experiments, all animals received care in compliance with the guidelines outlined in the Guide for the Care and Use of Laboratory Animals and all procedures were approved by the Animal Care and Use Committee of Shanghai Jiao Tong University.

1.13 Ex vivo fluorescence imaging. Ex vivo fluorescence imaging experiments were performed on a ZKKS-Mulaurora imaging system (Guangzhou ZhongkeKaisheng Medical Technology Co., Ltd, China). In this study, DOX was used as fluorescence probe which was physically incorporated in the NPs. The DOX loaded NPs were prepared as below: water soluble DOX·HCl was first converted to water-insoluble base (DOX) as described previously.^[1] 2.5 mg PEG-PCDA (or Biotin-PEG-PCDA) and 0.10 mg DOX were dissolved in 1 mL of methanol and chloroform mixture (12.5 : 87.5 (v/v)). 5 mL of deionized water was slowly poured into the solution and then sonicated at 200 w for 2 min, the power was pulsed for 5s every 30 s to minimize temperature increase. After that, the organic solvent was evaporated by rotary evaporation at 40 °C. The formed NPs solution was obtained by centrifugation at 4000 rpm for 20 min to remove the aggregated particles. The DOX-loaded NPs and free DOX·HCl were injected into mice bearing EMT6 tumor via lateral tail vein (DOX dose: 0.5 mg/kg), respectively. The mice were sacrificed at 2, 6, 12 and 24 h post-injection. After which, the major organs or tumors were harvested, and the tissues were imaged on the ZKKS-Mulaurora imaging system immediately. The ROI (regions of interest) analysis was measured under the assistance of Winmi software.

1.14 In vivo antitumor efficacy evaluation. Female Kummung mice were obtained from SLRC Laboratory Animal Company (Shanghai, China) and used at 6 weeks of age. 0.2 mL EMT6 cells ($1.0 \times 10^7/\text{mL}$) were injected subcutaneously and inoculated into female Kummung mice on day 0. On day 5, the tumors grew up to about 300 mm^3 , the mice were divided into five groups (6 mice per group) in a way to minimize weight and tumor size differences among the groups. Five groups were intravenously injected with about 0.2 mL of free Cur, Cur-loaded PAE-PEG NPs, PEG-PCDA NPs or Biotin-PEG-PCDA NPs solution (Cur or equivalent dose: 10 mg/kg) daily for nine consecutive days. The blank control group was treated with physiological saline. Free Cur was dissolved in cremophor EL (polyoxyl 35 castor oil) and dehydrated alcohol (1:1, v/v) and diluted with physiological saline to get a Cur solution for injection. The body weight and tumor volume were measured every two days. The tumor volume was estimated using the formula: $V = a \times b^2/2$, where “a” is the length of the major axis, and “b” is the length of the minor axis. On day 14, the animals were sacrificed by cervical dislocation. The tumor tissue was collected for histopathology and immunohistochemistry analyses. The inhibition rate of tumor growth (IRT) was calculated. The IRT can be quantified from the mean tumor weight (MTW) difference against the negative control via the equation:

$$\text{IRT} = [\text{MTW of control} - \text{MTW of treatment}] / [\text{MTW of control}] \times 100\%$$

1.15 In vivo antitumor efficacy evaluation of the DOX loaded Biotin-PEG-PCDA NP.

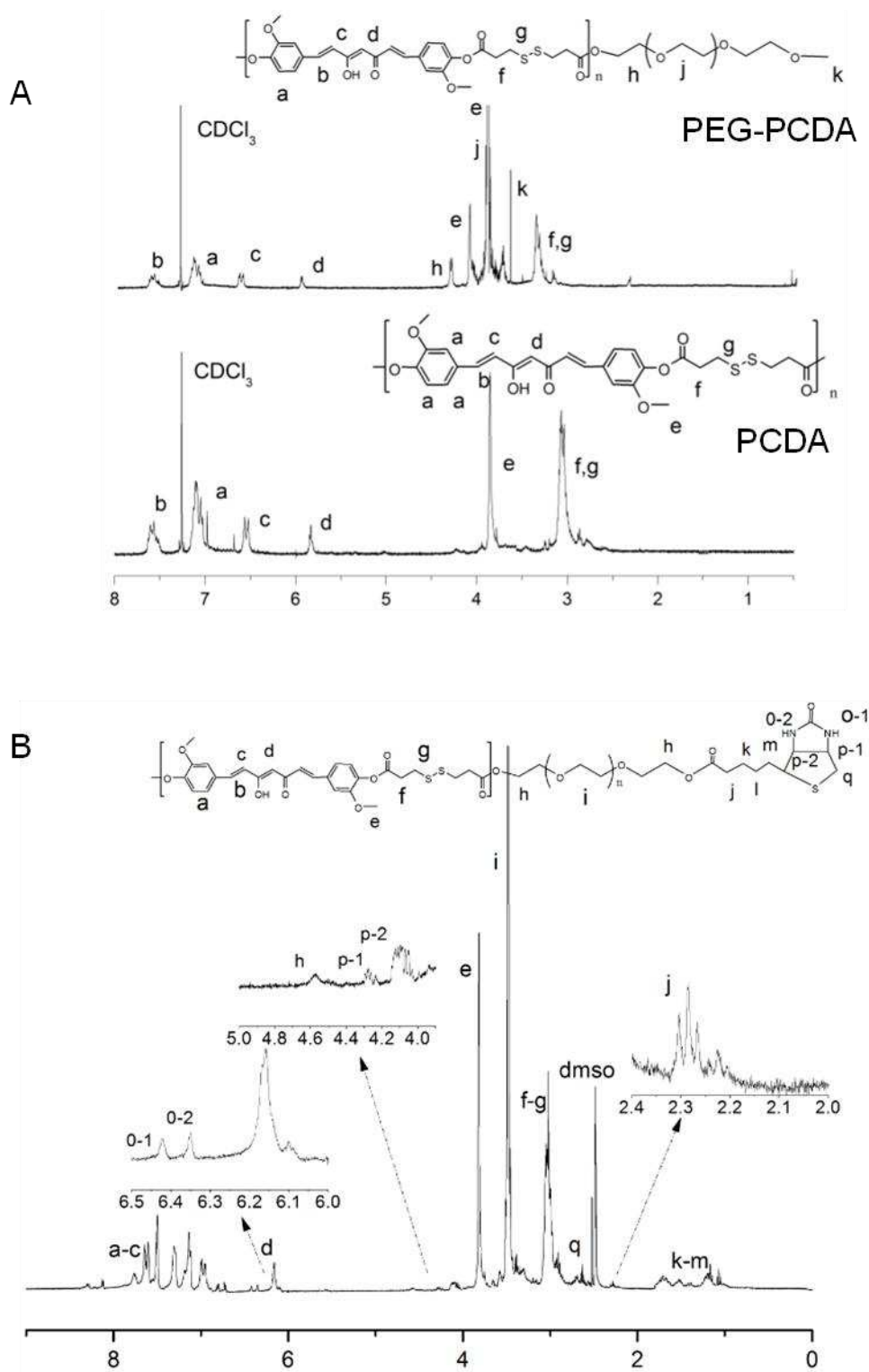
Doxorubicin hydrochloride was first converted to its hydrophobic free base using a previous protocol [1]. The DOX-loaded Biotin-PEG-PCDA NP was prepared by using an emulsion solvent evaporation method. In brief, a solution containing 10 mg of Biotin-PEG-PCDA and 2 mg of DOX in 3 mL of methanol/chloroform solution (12.5:87.5 v/v) was added into 10 mL water to form an oil-in-water emulsion. The emulsification was carried using a probe-type sonicator (Soniprep 150, Sanyo) under an ice bath at 200 w for 5 min, the power was pulsed for 5 s every 30 s to minimize increases in temperature. After that, the organic solvent was evaporated by rotary vacuum at 40 °C. The resulting suspension was centrifuged at 4000 rpm for 20 min to remove any aggregated particles and unencapsulated free DOX. The obtained clear supernatant was then lyophilized to obtain the DOX loaded Biotin-PEG-PCDA NP powders.

The same EMT6 tumor bearing mice model was established and used for the in vivo evaluation as above. On day 3, the tumors grew up to about 100 mm^3 , the mice were divided into four groups (6 mice per group) in a way to minimize weight and tumor size differences

among the different groups. Four groups were intravenously injected with about 0.2 mL of free doxorubicin hydrochloride (DOX), a physical mixture of free DOX and the Biotin-PEG-PCDA polymer (DOX+Biotin-PEG-PCDA), DOX-loaded Biotin-PEG-PCDA NP solution (DOX/Biotin-PEG-PCDA NP) once every two days for 4 times consecutive administration. The dosage of DOX was 2 mg/kg and the dosage of Biotin-PEG-PCDA was 14.7 mg/kg (equivalent of 4 mg/kg of Cur). The blank control group was treated with physiological saline. The mixture of free DOX and the Biotin-PEG-PCDA polymer were dissolved in cremophor EL (polyoxyl 35 castor oil) and dehydrated alcohol (1:1, v/v) and diluted with physiological saline for injection. The body weight and tumor volume were measured every two days. The tumor volume was estimated using the formula: $V = a \times b^2/2$, where “a” is the length of the major axis, and “b” is the length of the minor axis. On day 10, the animals were sacrificed by cervical dislocation. The tumor tissue was collected. The tumor volume change (TVC)s was calculated. The inhibition rate of tumor growth (IRT) was also calculated as above.

1.16 Histological and immunohistochemical evaluation. Tumor tissues were collected, fixed with paraformaldehyde overnight, and then embedded in paraffin. The paraffin-embedded tumor tissues were cut at 5 μm thickness, and stained with hematoxylin and eosin to assess histological alterations by Olympus BX 51 microscope. Tumor tissue sections were also used for Ki-67 staining by the labeled streptavidin-biotin method. The primary antibody and secondary antibody were rat anti-mouse monoclonal antibody Ki-67 (Gene Tech) and biotinylated goat anti-rat immunoglobulin (BD Biosciences Pharmingen), respectively. Cellular apoptosis assay was carried out by reacting sliced tissues with terminal transferase dUTP nick end labeling (TUNEL) assay (Roche) according to the protocol from the manufacturer.

1.17 Evaluation of in vivo CD31, VEGF and COX-2 levels in tumor tissues. CD31, VEGF and COX-2 expressions in tumor tissue were investigated by immunohistochemical staining to evaluate the antiangiogenesis effect. Briefly, tumor tissue sections were stained with rat anti-mouse CD31 polyclonal antibody (1:50; BD Pharmingen USA), washed twice with PBS, and followed by incubating with a Cy3-conjugated second antibody (Jackson, USA). To study VEGF and COX-2 expression, tumor sections were deparaffinized in xylene. After blocking endogenous peroxidase and nonspecific antibody binding, rabbit polyclonal anti-COX-2 antibody or rabbit polyclonal anti-VEGF antibody was diluted at a ratio of 1:200 in 1% bovine albumin-containing PBS and the tumor sections were incubated for 1 h at room



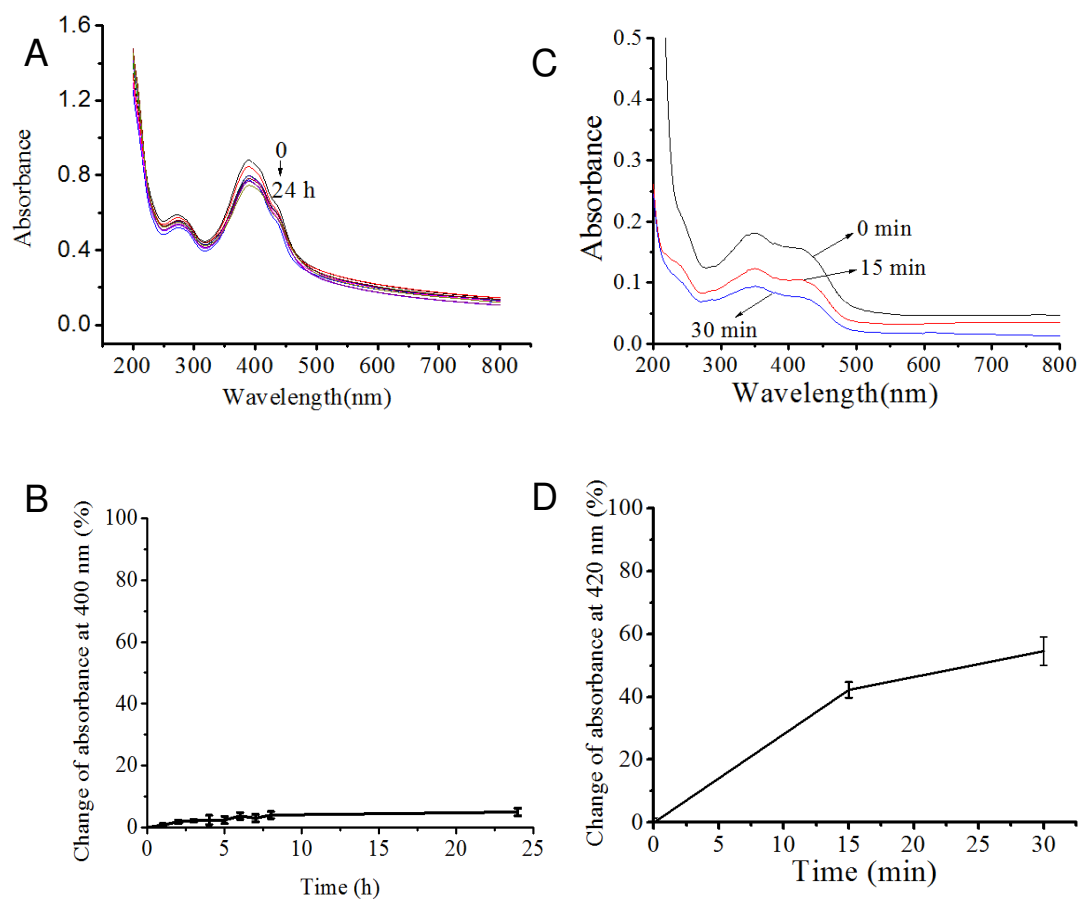


Figure S3. UV-visible spectra of the Biotin-PEG-PCDA and curcumin in PBS at pH of 7.4. (A) UV-visible spectra of Biotin-PEG-PCDA dissolved and kept in PBS for 0, 1, 2, 3, 4, 5, 6, 7, 8 and 24 hours; (B) Change of the absorbance at 400 nm for Biotin-PEG-PCDA in PBS vs. time; (C) UV-visible spectra of curcumin dissolved and kept in PBS for 0, 15 and 30 min; (D) Change of the absorbance at 420nm of curcumin in PBS vs. time.

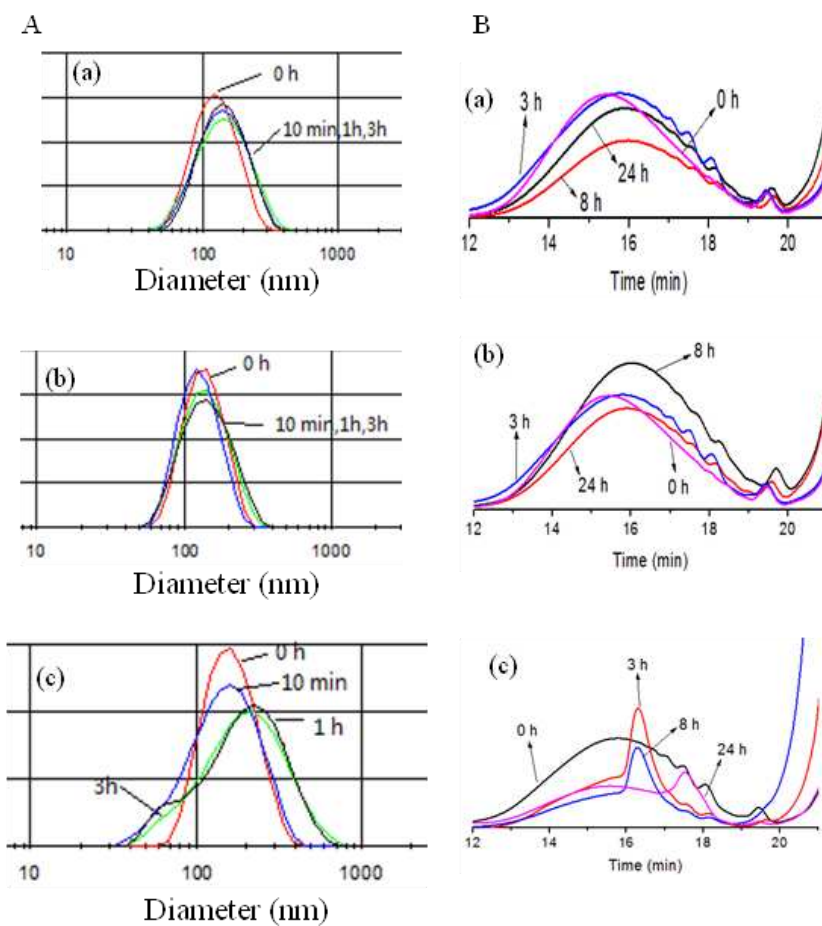


Figure S4. Dynamic Light Scattering (A) and GPC (B) profiles of the Biotin-PEG-PCDA NP after exposure to PBS (10 mM phosphate, 150 mM NaCl, pH 7.4) with different GSH concentrations: 0 (a), 10 μM (b) and 5 mM (c).

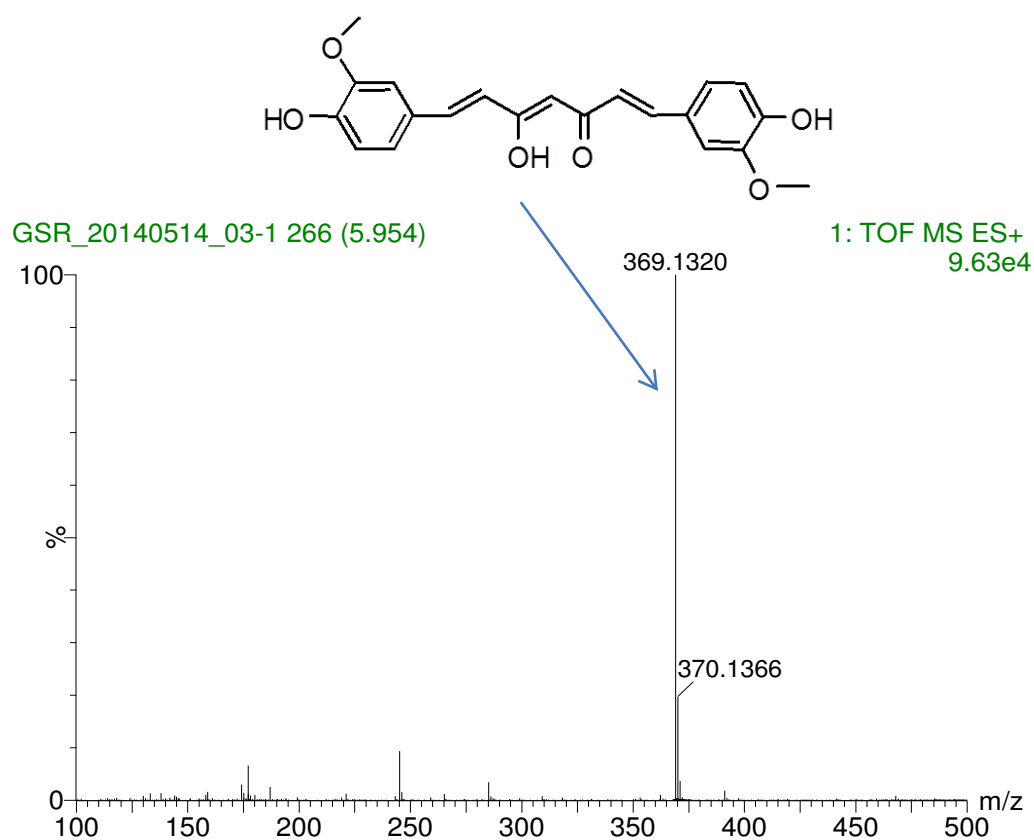


Figure S5. Typical LC-HR-MS spectrum showing the degraded specie (Cur) and its assignment ($M + H$)⁺ peaks after treatment of the biotin-PEG-PCDANP with 5 mM glutathione and esterase (100 U) in PBS for 24 hours.

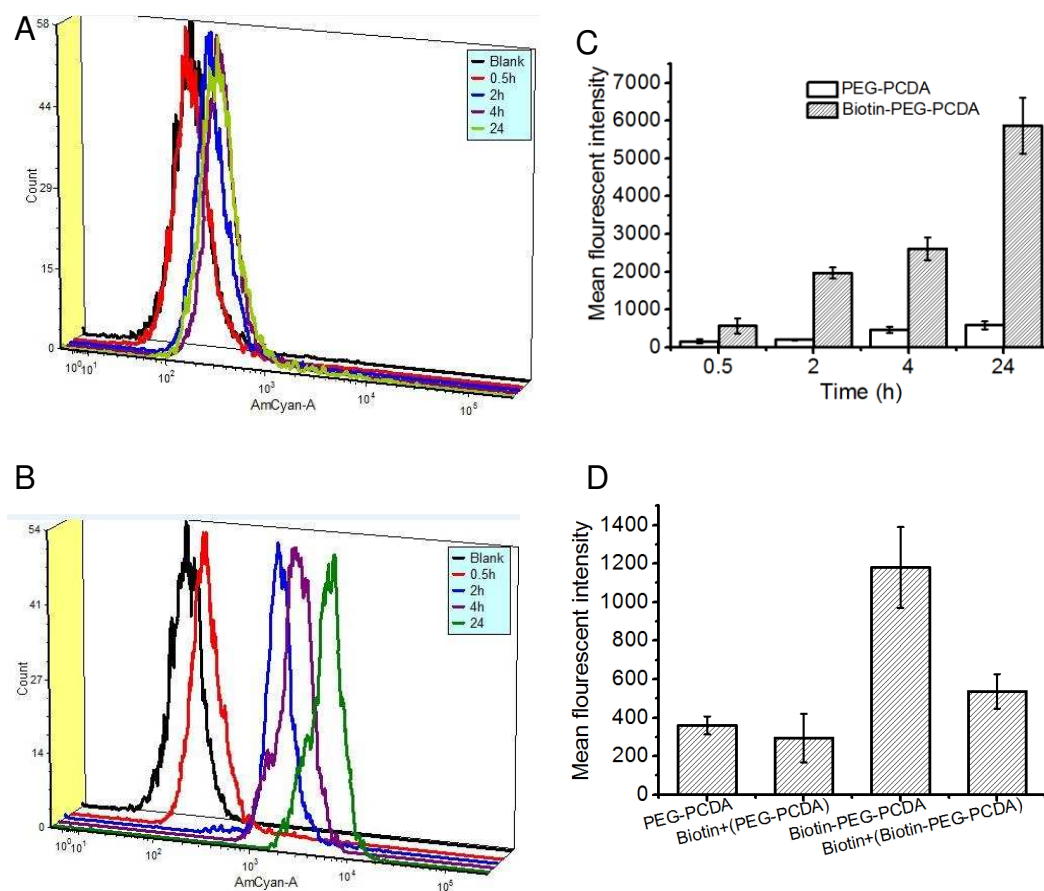


Figure S6. Flow cytometry investigation of uptake of the PEG-PCDA and Biotin-PEG-PCDA NPs by HeLa cells. **A** and **B**: Cur fluorescence intensity histograms for HeLa cells after incubation with the PEG-PCDA and Biotin-PEG-PCDA NPs for 0.5, 2, 4 and 24 h, respectively. **C**: Evolution of mean Cur fluorescence intensity for HeLa cells after incubation with the PEG-PCDA and Biotin-PEG-PCDA NPs as a function of time. **D**: Mean fluorescent intensities of HeLa cells after 1.5 h incubation with the PEG-PCDA NPs, 2 mM biotin + PEG-PCDA NPs, Biotin-PEG-PCDA NPs, and 2 mM biotin + Biotin-PEG-PCDA NPs.

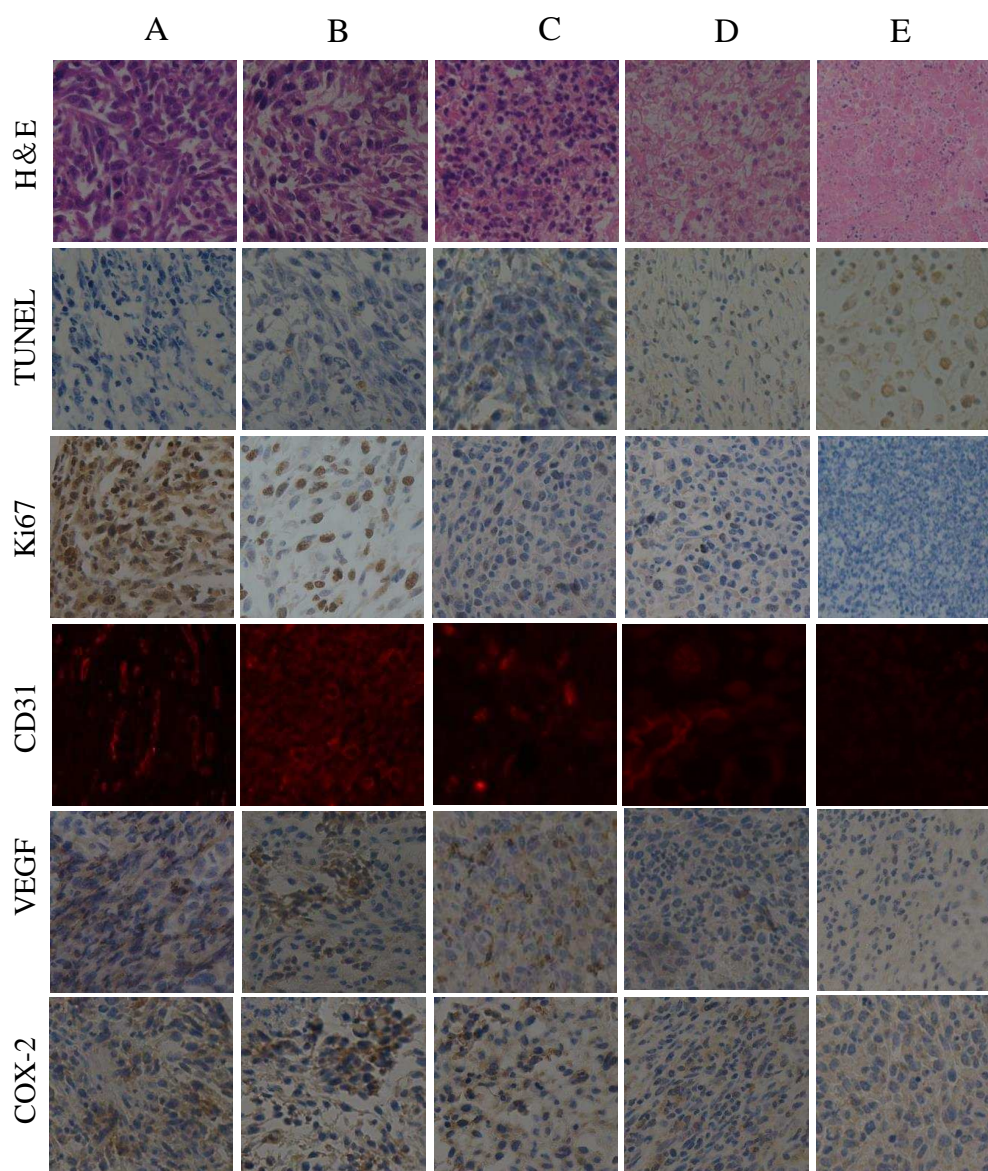


Figure S7. The H. & E., TUNEL, Ki-67, CD31, VEGF and COX-2 photographs of tumor tissues of Kunming mice burdened with EMT6 tumor after being treated by intravenous injection with saline (**A**, negative control), free Cur (**B**), the Cur/PAE-PEG NPs (**C**), the PEG-PCDA NPs (**D**), and the Biotin-PEG-PCDA NPs (**E**) at a daily Cur or equivalent dose of 10 mg/kg for 9 consecutive days.

The H&E staining results showed that treatments with the Biotin-PEG-PCDA NPs resulted in most tumor cell necrosis. Treatments with both Biotin-PEG-PCDA and PEG-PCDA NPs caused significant apoptosis from the TUNEL photos. The Ki67 assay revealed a significantly reduced level of Ki67 in the Biotin-PEG-PCDA NP treated group compared to those of the PEG-PCDA NPs, Cur/PAE-PEG NPs, free curcumin and negative control groups.

Angiogenesis has a major role in tumor growth, dissemination and metastasis in solid and hematological tumors. Immunohistochemical assessment using a CD31 staining can be utilized for investigation of tumor vessels in tumor tissue. VEGF is a major pro-angiogenesis factor in tumor

microenvironment and COX-2 is involved in the regulation of VEGF-induced angiogenesis. Herein, we tested the CD31, VEGF, COX-2 expression levels in tumor tissue. Considerable amount of microvessels was clearly observed in the free Cur treated and negative control groups (shown in red fluorescence). In contrast, microvessels were much fewer in the Cur/PEG-PAE or PEG-PCDA NPs treated groups, and were the fewest (and in fact rarely observed) in the Biotin-PEG-PCDA NP treated group, confirming that the Biotin-PEG-PCDA NP had the greatest inhibition toward microvessel formation in tumors. Moreover, the VEGF and COX-2 expression levels were inhibited to a greater extent in the Biotin-PEG-PCDA, PEG-PCDA or Cur/PAE-PEG NP treated groups than those found in the free Cur and saline control groups. Taken together, it is clear that the Biotin-PEG-PCDA NP were very effective in inducing tumor apoptosis, inhibition of cell proliferation by providing effective anti-angiogenesis properties.

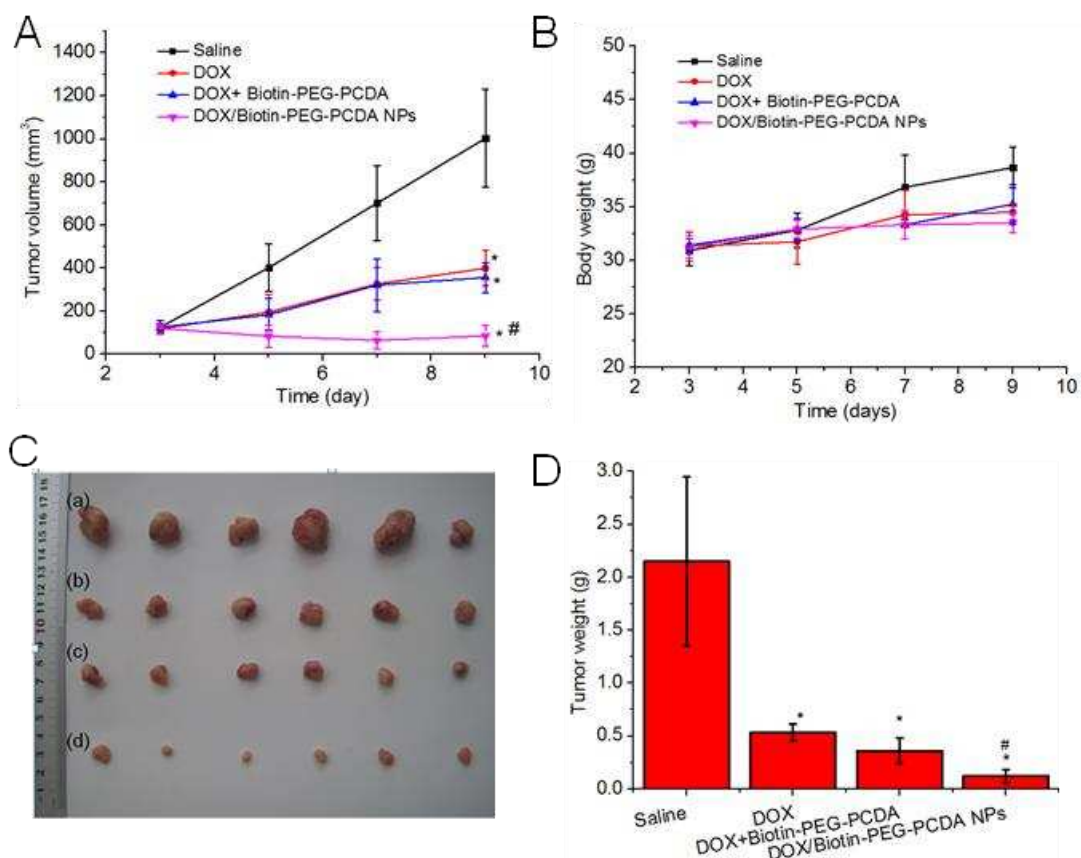


Figure S8. Changes of tumor and body weights of Kumming mice bearing EMT6 tumor with time (the treatments started on day 3). **(A)** Tumor volume v.s. time, * $p < 0.01$ compared to control group; $\Delta p < 0.01$ compared to free DOX group; **(B)** Body weights v.s. time; **(C)** photos of tumors at the end of the experiment: saline group **(a)**, free DOX group **(b)**, the physical mixture of free DOX and Biotin-PEG-PCDA polymer group **(c)**, the DOX loaded Biotin-PEG-PCDA NP group **(d)**; **(D)** Tumor weights at the end of the experiment after injection with the saline, free DOX, the physical mixture of free DOX and Biotin-PEG-PCDA polymer or DOX/Biotin-PEG-PCDA NP for 6 days. (significant difference, * $p < 0.01$ compared to control; # $p < 0.01$ compared to free DOX)

Part 3: Supporting Tables

Table S1. Characterization of the prepared polymers.

*Data in parenthesis: concentrations of equivalent curcumin

| polymer | Mn | PDI | Solubility in water ($\mu\text{g/mL}$) |
|-----------------|-------|-----|--|
| PEG-PCDA | 8930 | 1.5 | 360 (84*) |
| Biotin-PEG-PCDA | 9230 | 1.7 | 470 (127*) |
| PEG-PAE | 11080 | 2.4 | — |
| Curcumin | — | — | 0.25 |

Table S2. Physical parameters of the polymer nanoparticles used in this study

| nanoparticles | Size(nm) | PDI | Zeta-potential(mv) | Drug Loading(%) |
|-----------------|-----------------|-----------------|--------------------|-----------------|
| PEG-PCDA | 94.2 \pm 2.8 | 0.17 \pm 0.02 | -9.56 \pm 0.86 | 23 |
| Biotin-PEG-PCDA | 125.1 \pm 2.7 | 0.08 \pm 0.05 | -12.86 \pm 1.94 | 27 |
| Cur/PEG-PAE | 98.5 \pm 1.0 | 0.14 \pm 0.00 | -9.73 \pm 1.70 | 8 |